INTERNATIONAL JOURNAL OF CLIMATOLOGY
Int. J. Climatol. **22**: 87–106 (2002)
DOI: 10.1002/joc.711

INVESTIGATING THE LINK BETWEEN EARLY SEASON CARIBBEAN RAINFALL AND THE EL NIÑO+1 YEAR

A. ANTHONY CHEN* and MICHAEL A. TAYLOR
Department of Physics, University of the West Indies, Mona, Jamaica

Received 14 July 2000
Revised 25 June 2001
Accepted 6 July 2001
Published online 31 January 2002

ABSTRACT

The Caribbean rainfall season is best characterized by its bimodal nature, with an initial peak in May–June and a second more prominent one in September–October. This allows for a convenient division into an early and a late rainfall season. In this study we examine the rainfall patterns of the early rainfall season (mid April to July) for links with El Niño–Southern Oscillation (ENSO) events. Whereas traditionally ENSO events have been identified with dry conditions during the later Caribbean rainfall season, recent research suggests a second signal that manifests itself as a wet early rainfall season of the year of ENSO decline (the El Niño+1 year). Two leading empirical orthogonal function modes of early season Caribbean rainfall are examined for evidence of this. Strong correlations are shown to exist between the first mode and wintertime equatorial Pacific anomalies. The first mode explains nearly half of the early season variability. The idea that the wintertime Pacific anomalies alter the early Caribbean rainfall season via the warm spring sea surface temperature anomalies they induce in the north tropical Atlantic is also investigated. An atmospheric general circulation model is also used to show that, when warm/cold anomalies exist across the north tropical Atlantic, this results in a large-scale atmospheric circulation that is more/less favourable to rainfall production over the Caribbean.

KEY WORDS: Caribbean; rainfall SST; El Niño; ENSO; EOF; AGCM

1. INTRODUCTION

The Caribbean rainfall season, spanning April to November, is bimodal in nature with an initial peak between May and July and a second between September and October. This bimodality allows for a convenient division into an early (April–July) and a late (August–November) rainfall season (Figure 1) with the latter characterized by more abundant rainfall with the passage of tropical storms and hurricanes.

In this paper we present results from an investigation of early season Caribbean rainfall. The impetus for studying the Caribbean rainfall onset months includes: (i) a lack of studies devoted to interannual variability of Caribbean rainfall during this period; (ii) a recent history of devastating floods in sections of the Caribbean during this period (Fernandez, 1996); and (iii) the calamitous effects of a protracted dry season (i.e. December through July) during periodic absences of May–June rains (Brown, 2000); (see Figure 1 again). The paper is divided into two parts, each with a distinct investigative task.

In the first part we confirm via data analysis the presence of an El Niño–Southern Oscillation (ENSO) signal in early season Caribbean rainfall. Given the predictability of ENSO events seasons in advance, identifying such a relationship enhances the possibility of predicting anomalous early rainfall seasons. We establish statistically that the likely propagation of the ENSO signal into the Caribbean is via a spring warming of the north tropical Atlantic (NTA) sea surface induced by a warm equatorial Pacific the previous winter. The

* Correspondence to: A. Anthony Chen, Department of Physics, University of the West Indies, Kingston 7, Jamaica;
e-mail: achen@uwimona.edu.jm

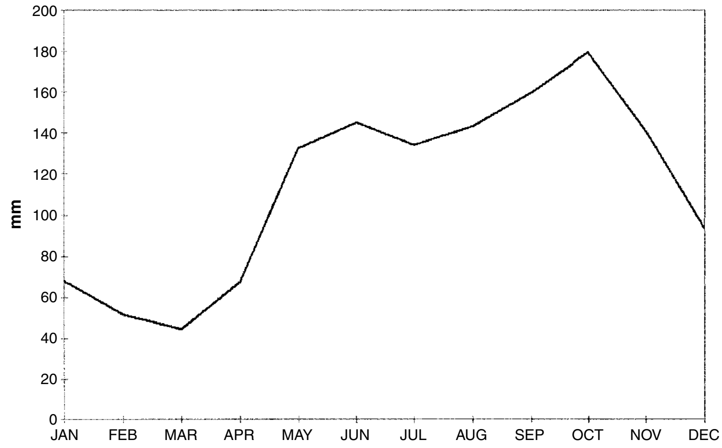

Figure 1. Precipitation climatology of the Caribbean (mm month^{-1}) showing the early (AMJJ) and late (ASON) rainfall season

paper extends the limited body of work devoted to Caribbean–ENSO relationships, but is distinct given its focus solely on the early season.

The second part of the paper examines how both Caribbean rainfall amounts and the large-scale atmospheric circulation pattern of the early season are altered under prescribed sea surface temperature (SST) conditions in the tropical Pacific and Atlantic akin to those of the year of the El Niño decline (hereafter termed the El Niño+1 year). We establish that, during the early season following the winter peak in equatorial Pacific SST anomalies, i.e. the El Niño+1 year, the large-scale tropospheric structure over and around the Caribbean is biased towards one conducive to convection (largely due to the warm NTA mentioned previously). Here, use is made of an atmospheric general circulation model (AGCM). The use of a model represents a dimension missing from previous investigations of Caribbean rainfall.

The background to the study is offered in Section 2, and descriptions of the data, methodology and model used are given in Section 3. Statistical and model results are presented in Sections 4–6. In Section 7 we offer a discussion of the results, including a mechanism by which the early season rainfall anomalies arise during the El Niño+1 year. A summary of the major findings is given in Section 8.

2. BACKGROUND

A number of studies have addressed year-to-year fluctuations in Caribbean rainfall, with much emphasis placed on establishing a connection to ENSO. Hastenrath (1976) showed that rainfall was *negatively* correlated with SSTs in the eastern equatorial Pacific, and Ropelewski and Halpert (1986, 1987, 1989, 1996), Rogers (1988), and Aceituno (1988a) further contribute to the development of the 'dry Caribbean–warm Pacific' relationship based on data studies. A common feature of these studies is a focus on the *latter* portion of the rainfall season (i.e. July–November), given its abundance of rainfall and its coincidence with peak hurricane activity.

Recently, Chen *et al.* (1997), Taylor (1999) and Giannini *et al.* (2000) addressed rainfall rates in the early part of the rainy season. Their studies indicate a strong *positive* relationship between early season Caribbean rainfall and the El Niño event (Figure 2), contrary to the negative ENSO relationship traditionally proffered. That is, the tendency is for a *wetter* Caribbean during the early season due to an El Niño event. Chen *et al.* (1997) also suggest that the converse, i.e. of a dry Caribbean from April to July, during La Niña events is also true. In examining the early season rainfall anomalies, the studies also establish that: (i) during the periods of El Niño related early season rainfall anomalies, concurrent warm SST anomalies (SSTAs) exist in the NTA (Taylor, 1999; Giannini *et al.* 2000); (ii) the early season rainfall anomalies occur during the El Niño+1 year (Chen *et al.* 1997; Taylor, 1999).

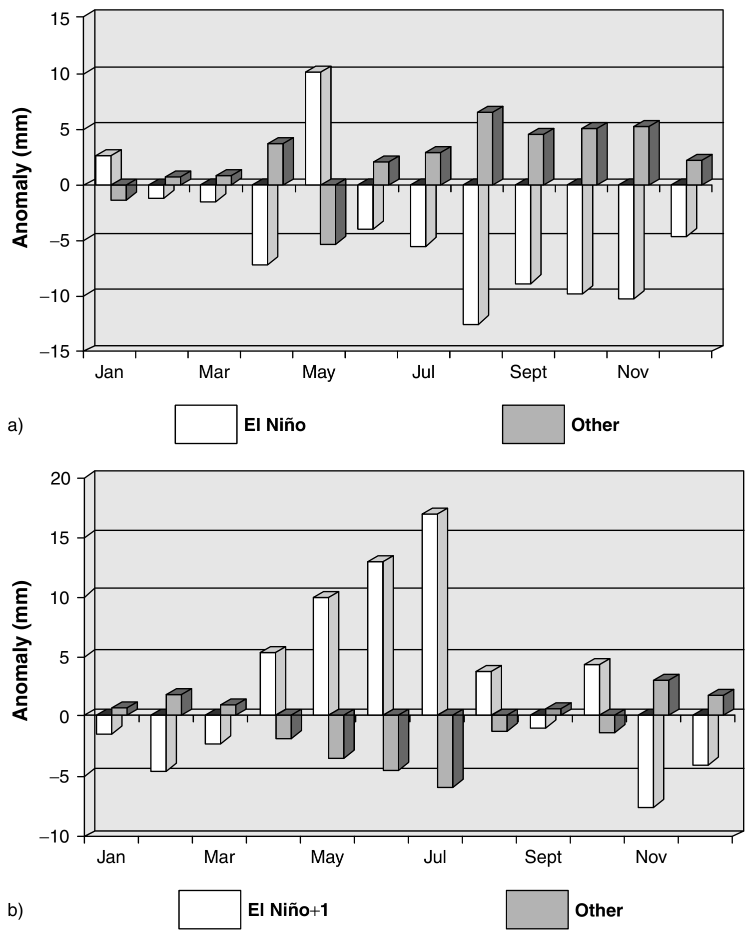

Figure 2. (a) The mean monthly Caribbean precipitation anomaly for El Niño years (white) versus other years (shaded), showing negative correlation between Caribbean rainfall and Pacific SSTs found in earlier studies. (b) As in (a) but for El Niño+1 years (white) versus other years (shaded), showing the tendency towards a wetter Caribbean in El Niño+1 years

The alteration of Caribbean and NTA SSTs in the face of an ENSO event (idea (i) above) is explored by Curtis and Hastenrath (1995), Enfield and Mayer (1997) and Chen *et al.* (1997). All show that NTA SSTs (inclusive of the Caribbean) lag those of the equatorial Pacific by 4 to 5 months. This ensures that warm anomalies engulf the NTA and Caribbean at least through boreal spring and during the early Caribbean rainfall season following an ENSO event. That these NTA SSTAs can in turn influence Caribbean rainfall is suggested by the robust relationship between SSTs and easterly wave development (Gray, 1968; Carlson, 1971; Emanuel, 1987) — easterly waves being the primary source of Caribbean rainfall. We investigate the relationship between ENSO, the warm NTA SSTAs and early season Caribbean rainfall anomalies.

In contrast, the restriction of the early season anomalies to the El Niño+1 year (idea (ii) above) is seen as a consequence of a noted relationship between Caribbean rainfall and concurrent SSTAs in the tropical Atlantic and tropical Pacific. Enfield and Alfaro (1999) show via singular value decomposition (SVD) analysis that, in the face of a warm tropical Atlantic–cool tropical Pacific scenario, there is a tendency for enhanced rainfall over the Caribbean and Central America and an early onset to the rainy season. A similar configuration is noted by Taylor (1999) to be typical of an El Niño+1 year, as a declining El Niño ensures a cooler equatorial Pacific, even as the NTA is warming due to the SST lag relationship outlined previously. (Note again the importance of the ENSO-induced NTA spring warming for the early season rainfall anomalies.) It is likely, then, that it is the confluence of favourable SST conditions in both tropical ocean basins during the El

Niño+1 year that yields the early season Caribbean rainfall anomalies. We investigate the effect of various tropical SSTA scenarios on the large-scale circulatory structure of the Caribbean, for bias toward wet or dry conditions.

3. DATA, METHODOLOGY AND MODEL

3.1. Data

The data set of Caribbean precipitation (hereafter referred to as the University of the West Indies (UWI) data set) consists of monthly averaged station data and was compiled from the Climate Prediction Center's Climate Anomaly Monitoring System (CAMS) station data for January 1851 through to September 1994, and the Carbon Dioxide Information Analysis Center (CDIAC) Global Historical Climatology Network data base (Vose *et al.*, 1992) for October 1832 through to October 1990. Duplicate data were ignored and the combined data set was gridded in the Grid Analysis and Display System (GrADS) R40 format using an area weighting average. This allowed for extrapolation over the Caribbean Sea. The data set spans the period 1832–1994, but the period of investigation was restricted to January 1921–December 1986, during which time the number of Caribbean stations regularly reporting precipitation events exceeded 100. The climatology averaged over the investigation period was removed from the dataset.

The UWI data set was compared with the data of Xie and Arkin (1997) by calculating the correlations between derived time series of area-averaged precipitation anomalies from each dataset for 12 sub-regions shown in Figure 3. The Xie–Arkin data consists of merged gauge, satellite and numerical model estimates of global precipitation for the period 1979–96. Its limited time span precluded its use in the study. Correlations exceeded 0.75 in 9 of 12 sub-regions for the 15 years of overlap, with the exceptions being sub-regions 5, 10 and 11, where values of 0.65 or higher were attained. All correlations were significant at the 99% confidence level.

Though of finer resolution than the $5^{\circ} \times 5^{\circ}$ Xie–Arkin data set, the UWI precipitation data set is still too coarse to distinguish inhomogeneities across sharp orographic features in the region. As such, the results

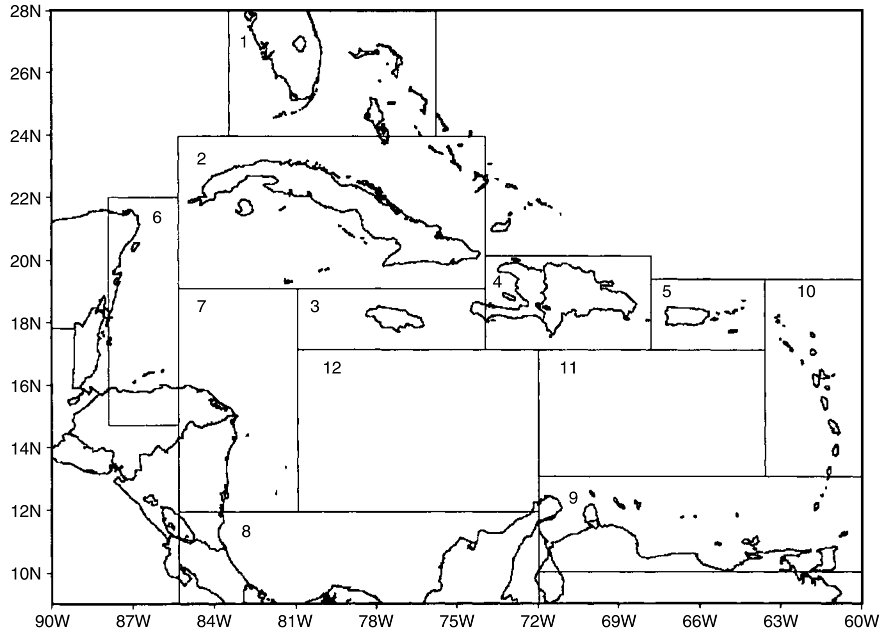

Figure 3. The Caribbean region. For the EOF analysis the region was divided into 12 sub-regions, also indicated in the diagram

obtained in this study are representative only in a large-scale sense, and do not speak of relationships on smaller scales where orography may be important.

The SST data used in the study was from the Hadley Centre GISST 2.2 ($1^\circ \times 1^\circ$) monthly global data set (Parker *et al.*, 1995) spanning 1903 to 1994.

3.2. Statistical analysis

Empirical orthogonal function (EOF) and spectral analyses were both used to elicit the primary modes of early season rainfall variability. For the EOF analysis of the May–June–July (MJJ) precipitation anomaly, the region was again subdivided into the 12 sub-regions (Figure 3), and the time series of anomalous early season rainfall for each sub-region (i.e. averaged over the region and over MJJ) extracted. Except for sub-regions 11 and 12, the regions were chosen to encompass entirely a country or set of smaller islands known to exhibit similar rainfall regimes. Regions 11 and 12 were chosen to be approximately the same size as the other regions.

Following Kutzbach (1967), a matrix of the anomalous precipitation for each of the 12 sub-regions times 66 years of data (1921–86) was created, and the EOF analysis done. The matrix is such that an element f_{ij} represents the anomalous early season rainfall in the ith sub-region for the jth year. The result of the technique is a decomposition of the MJJ rainfall anomalies into modes of decreasing explained covariance. Each mode is characterized by a singular vector describing the spatial pattern of weights (loadings) for the early season rainfall and a series of expansion coefficients describing the weighting of the mode in the temporal domain.

Correlations were then calculated between the time series of the expansion coefficients of the leading modes, i.e. those explaining most early season rainfall variance, and tropical Atlantic and Pacific SSTA indices. This allowed us to infer characteristics about the relationship between early season Caribbean rainfall and each oceanic basin. Throughout the analysis, correlations said to be statistically significant are significant at the 95% level or higher. Significance is determined by the random phase method (Ebisuzaki, 1997), which accounts for serial correlation in the data.

3.3. The model

To determine if and how the large-scale atmosphere is biased under particular SST configurations of the tropical Atlantic and Pacific, we use an AGCM. Since tropical circulations (Hadley and Walker) are mainly determined by changes in boundary conditions at the Earth's surface (Shukla, 1993), the time mean tropical circulation and rainfall become predictable provided a correct prescription of the boundary conditions (SST and sea ice) are given in the model (Shukla and Fennessy, 1988).

The model used is the Center for Ocean Land Atmosphere Studies (COLA) T30 AGCM, which was installed and run on a Convex C3440 computer at the University of the West Indies. The COLA AGCM is a modified version of the National Center for Environmental Prediction (NCEP) global spectral model (Sela, 1980), with modifications, initialization procedures and boundary conditions as described in Kinter *et al.* (1988). It is vertically discretized into 18 sigma levels and incorporates a simple biosphere model (Xue *et al.*, 1991) to provide lower boundary conditions over the land portions of the model. The SST and ice data-sets used in the model were prepared by COLA using respectively the Hadley Centre GISST 1.0 ($1^\circ \times 1^\circ$) from 1948 to 1994, and the Climate Prediction Center (CPC) $2^\circ \times 2^\circ$ blended data set (Reynolds, 1988).

Model validation for use in the Caribbean is documented by Taylor (1996) for the months of March through to June. In brief, he suggests the model as being a good simulator of the mean climate of the region for the 4 month period, as it captures the expected mean spatial and temporal trends for major climatic variables. This includes monthly increases in rainfall amounts due to the onset of a rainy season in April, and the gradient in precipitation totals from the northwest to southeast Caribbean. Our subsequent simulations show the model to overestimate Caribbean precipitation in the following month of July, with a tendency to place areas of maximum precipitation well away from those noted from observations. This latter deficiency suggests the model's inability to capture adequately the mid-season decrease in precipitation characteristic of the region in July (Figure 1). Magaña *et al.* (1999) in describing the 'midsummer drought (MSD)' over the west coast of southern Mexico and Central America, attribute it to diminished down-welling solar radiation (due to increasing cloud amount) and stronger easterly winds. If a similar mechanism accounts for the MSD in the Caribbean, then the model's inability to capture it might lie in an inadequate sub-grid-scale cloud prescription scheme and feedback mechanism. Although the atmospheric circulation is reasonably represented in the model, the same is not necessarily true for cloud amounts.

As with the data-sets used, the model resolution is too coarse to offer an insight into the climate of individual Caribbean territories due to their often sub-grid-scale size.

4. CONFIRMING THE ENSO–EARLY SEASON CARIBBEAN CONNECTION

The first two leading modes of the EOF analysis explain 46% and 16% of the total early season rainfall variance. The spatial patterns and corresponding expansion coefficients for each are depicted in Figure 4 and Figure 5 respectively. Based on the Kaiser (1960) criterion and the scree test (Cattell, 1966), the third and fourth modes, which respectively explained 10% and 8% of the variance, could be retained. These modes were, however, dominant only on the fringes of the Caribbean region (regions 6 and 9 for the third mode and region 8 for the fourth mode) and are not discussed in this paper.

4.1. The Caribbean Basin (CB) mode

The spatial pattern of the leading mode (Figure 4(a)) reveals a homogeneous Caribbean basin, with similar signature in 11 of the 12 sub-regions. Only in the far northern basin (the southern tip of Florida and the northernmost Bahamian isles) is there an opposite sign, though the magnitudes of the spatial loadings in the rest of the basin decrease significantly north of 20 °N. Because Figure 4(a) shows sub-regions 3, 4, 5, 10, 11 and 12 (southern Cuba, Jamaica, Hispaniola and the northern Leeward Islands) as the centres of action (i.e. with largest spatial loadings), the first mode is seen as characterizing the variability of the majority of the Caribbean isles and is called the CB mode.

The expansion coefficients for the CB mode (Figure 4(b)) show a significant decadal variability, upon which the interannual signal is superimposed. Amidst yearly fluctuations in magnitude and sign are stretches of predominantly wet (1930s, early 1940s) and dry (early 1920s, 1960s, 1970s) years — a tendency of Caribbean rainfall noted by Hastenrath (1976). The spectral analysis of the CB mode expansion coefficients (not shown) has maximum power at a periodicity of 16 years. The NTA SST exhibits a similarly strong decadal signal (Houghton and Tourre, 1992; Carton and Huang, 1994; Chang *et al*., 1997; Mehta and Delworth, 1998) with a fairly high degree of coincidence between phases of high/low SST and a wet/dry CB mode. We suggest that the dominance of the decadal signal hints at the importance of NTA SSTAs for Caribbean rainfall.

The secondary peak in the spectra of the CB mode is 5.5 years, and is similar to that often quoted as the period of the ENSO signal. To establish a relationship between El Niño occurrences and the CB mode, correlations were calculated between the latter's expansion coefficients and the NINO3 and NINO4 indices. NINO3 and NINO4 are time series of SSTA averaged over 90–150 °W, 5 °S–5 °N and over 150 °W–160 °E, 5 °S–5 °N respectively.

The NINO3 and NINO4 indices were first averaged over consecutive 3 month periods beginning in January, and correlations computed between the quarterly time series and the CB expansion coefficients, with the NINO indices leading the expansion coefficients by varying periods of up to a year. The correlations are listed in the first row of Table I, where quarters are indicated by the first letters of the months averaged, and a bracketed number indicates that the NINO quarter being correlated fell in either the previous (−1) or the same (0) year as the CB expansion coefficients. JAS(−1) therefore refers to the correlation between the CB mode expansion coefficients and the NINO index averaged over July to September of the previous year, and AMJ(0) indicates a correlation between the April–June NINO index and the CB expansion coefficients of the same year. Note that the correlation results presented in Table I cover the period 1956–86. In the course of the investigation it was discovered that marginally better correlations were achieved if only the last 31 years (1956–86) are used. One explanation is that data quality increased due to better collection techniques in the latter half of the century. The nature of the relationships indicated by the correlations, however, remained unchanged between the longer and shorter time series.

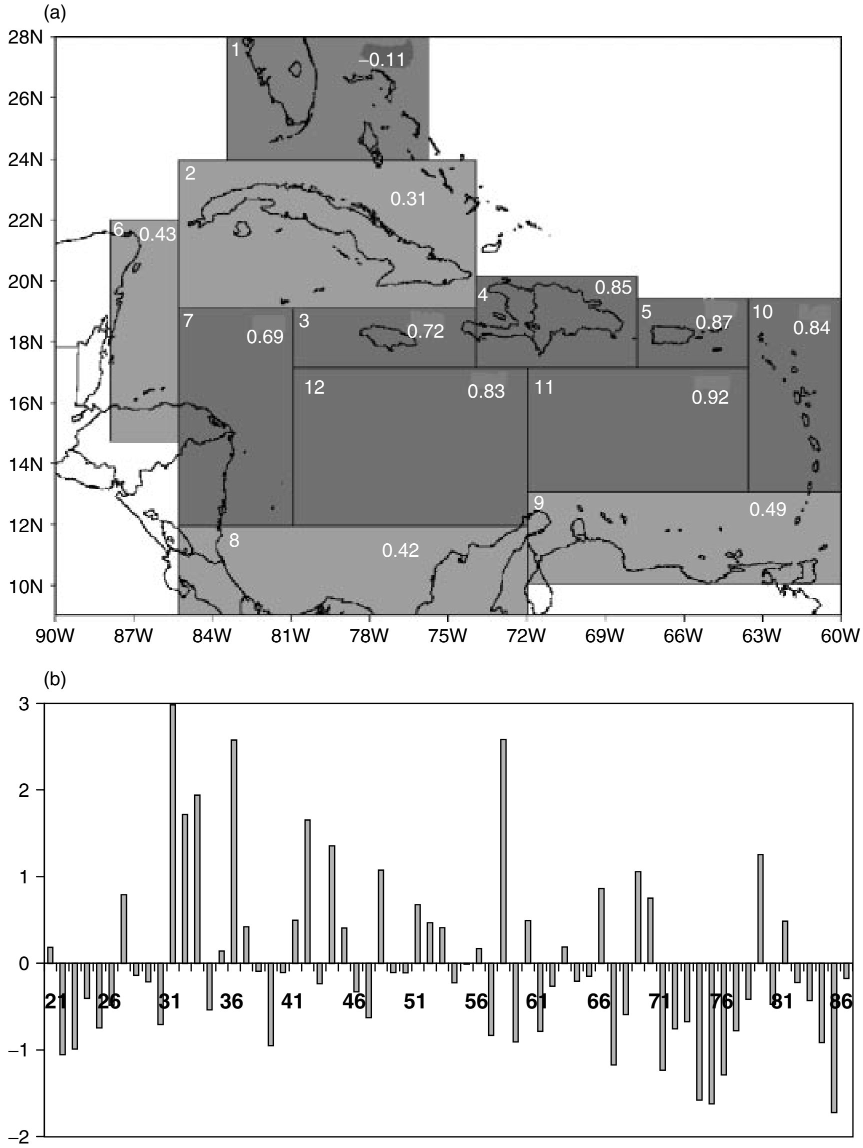

Figure 4. (a) The dominant (CB mode) EOF (46%) pattern and (b) the corresponding expansion coefficients for 1921–86 Caribbean rainfall departures. Darkest shading denotes largest loading and the loadings are listed in bold numbers in the upper right-hand corner of each box in (a)

Table I shows the dominant mode of early season precipitation variability (CB) to be significantly correlated with SSTAs of the equatorial Pacific the previous winter or early spring. For both the NINO3 and NINO4 indices, the best correlations (0.46 and 0.64 respectively) are obtained for JFM(0), with higher significant correlations between the Caribbean rainfall's leading mode and the NINO4 index. The sign of the correlation is such that a warm equatorial Pacific the previous winter is related to a wet early season. Subsequent analysis to isolate the 3 month period (not necessarily a calendar quarter) that yielded the best correlations with both indices showed that for NINO3 the preceding November–December–January (NDJ) and December–January–February (DJF) are as highly correlated as JFM in Table I, whereas in the case of NINO4 the best correlation remained in JFM. The robust correlations of Table I confirm the presence of an ENSO signal in early season Caribbean rainfall. The significant lag relationship between the NINO indices

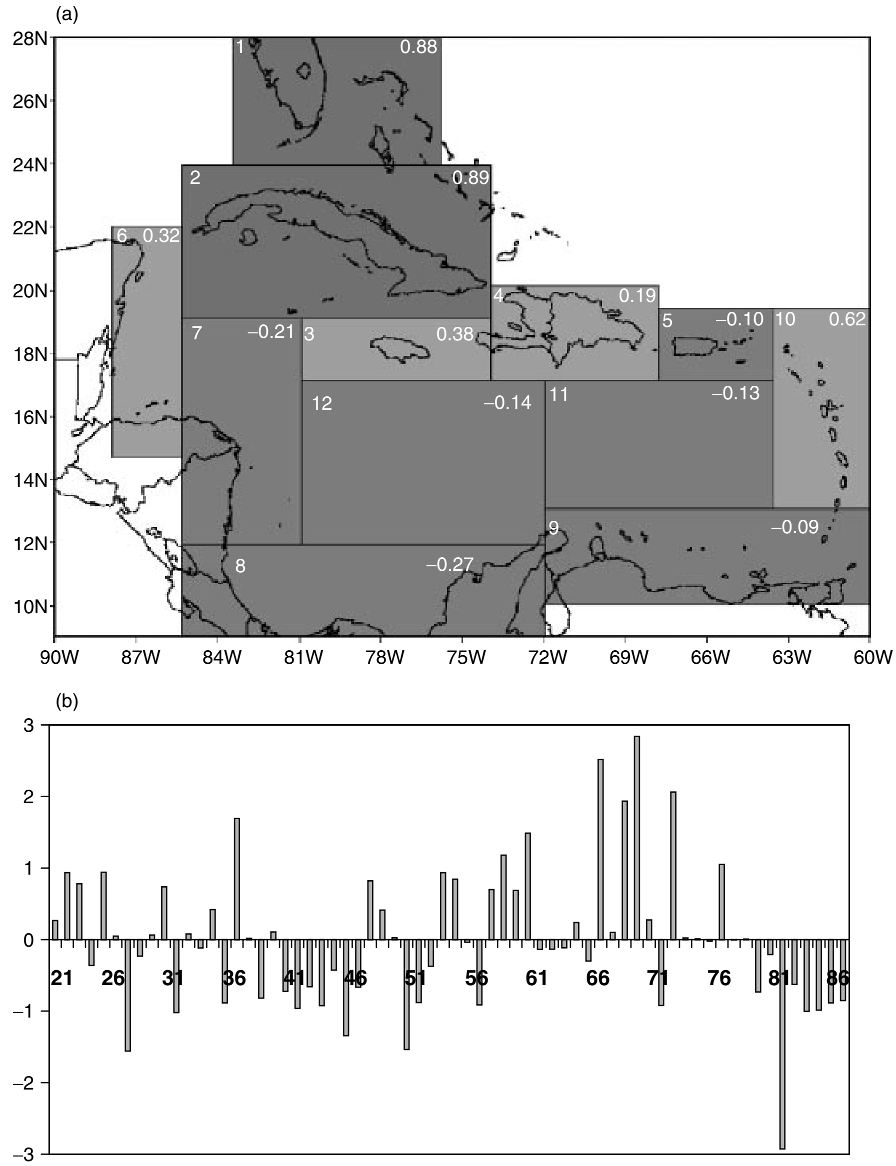

Figure 5. As in Figure 4, but for (a) the NC EOF mode (16%) and (b) the corresponding expansion coefficients

Table I. Correlations between the first two EOF modes (CB and NC) of early season Caribbean rainfall and the NINO3 and NINO4 indices for the period 1956–86

Mode	NINO3				NINO4			
	JAS(−1)	OND(−1)	JFM(0)	AMJ(0)	JAS(−1)	OND(−1)	JFM(0)	AMJ(0)
CB	**0.34**	**0.41**	**0.46**	0.26	**0.47**	**0.46**	**0.64**	**0.57**
NC	0.15	0.09	0.07	0.10	−0.02	0.13	0.31	**0.38**

Correlations significant at greater than the 95% level are given in bold.

Table II. As for Table I, but for correlations between the first two EOF modes (CB and NC) of early season Caribbean rainfall and the CSST index

Mode	CSST			
	JAS(−1)	OND(−1)	JFM(0)	AMJ(0)
CB	0.39	**0.47**	**0.53**	**0.69**
NC	−0.06	0.21	0.12	0.29

Correlations significant at greater than the 95% level are given in bold.

and the CB mode is consistent with an El Niño/La Niña altering MJJ rainfall via anomalous spring NTA SSTAs induced during the months leading up to and including the early season.

In Table II we present similar correlations to that of Table I, but for the CB mode expansion coefficients and quarterly time series of a Caribbean SSTA (CSST) index. Integral to the premise of an ENSO signal propagating into the Caribbean via its effect on NTA SSTs, must be the existence of a relationship between a warm/cold spring NTA and a wet/dry early season. The CSST index represents area-averaged anomalies (13–21 °N, 60–85 °W) over a domain chosen such that it (i) coincides with the Caribbean region of ENSO-induced spring anomalies (see Curtis and Hastenrath (1995) and Enfield and Mayer (1997)) and (ii) covers much of the region of largest spatial loading for the CB mode (see Figure 3). The AMJ CSST index is strongly and significantly correlated with both DJF NINO3 (0.64) and JFM NINO4 (0.68), suggesting that it captures the wintertime Pacific influence on the spring NTA SST. Table II shows that the CB mode is robustly correlated (0.69) with the CSST index for AMJ, with equally strong correlations for the months leading up to the early rainfall season. Given the known lag relationship between winter equatorial Pacific and the spring NTA SSTAs, Tables I and II together imply this as the likely means by which an ENSO event alters early season rainfall.

4.2. The north Caribbean (NC) mode

The spatial pattern of the second leading mode (Figure 5(a)) shows the largest loadings in sub-regions 1 and 2 (south Florida and northern Cuba), suggesting it largely characterizes the early season rainfall variability in this region. Consequently, this mode was called the NC mode. The pattern also depicts a tendency for groups of isles to vary in phase, a clustering trend also noted by Giannini *et al*. (2000) in their second and third combined PCA modes of rainfall climatology. Whereas sub-regions 3, 4 and 10 (Jamaica, Hispaniola and the Lesser Antilles, except Puerto Rico) are of the same signature as south Florida and northern Cuba, the southern basin (sub-regions 5, 7, 8, 9, 11 and 12) is in antiphase.

The time series of the NC expansion coefficients (Figure 5(b)) suggests (as for the CB mode) a strong decadal signal, with a tendency for dry conditions in the late 1930s, 1940s and late 1970s onwards, and wet conditions in the early 1920s, 1960s and early 1970s. Spectral analysis (not shown) confirms the dominance of this decadal component. We note also a contrast between the decadal wet and dry spells of the CB and NC modes between 1920 and 1980. On this time scale the two regions appear to operate in anti-phase.

Unlike the CB mode, there is no pronounced secondary peak of ENSO periodicity (periodogram not shown). Correlations of the expansion coefficients with the derived NINO3 and NINO4 indices (second row of Table I) also reveal little evidence of the lag relationship with wintertime Pacific anomalies seen in the CB mode. The only significant correlation is with AMJ NINO4 (0.38), indicating that if a Pacific influence does occur in the NC early season then it is due to concurrent equatorial Pacific SSTAs. The wintertime ENSO influence on the MJJ Caribbean basin rainfall (i.e. south of 20 °N) does not seem to alter the early season rainfall regime of the north Caribbean.

We see this also in the lack of a significant correlation between the NC mode and the CSST index for all quarters prior to and leading up to the early season (second row of Table II). The maximum correlation is 0.29 for AMJ of the same year. Interestingly, in both the work of Curtis and Hastenrath (1995) and Enfield and

Mayer (1997), there is a distinct demarcation of the northern edge of the warm NTA anomalies that develop in response to the warm winter Pacific. Though the NTA anomalies spread as far south as the equator, they do not progress north of 20 °N. This might suggest why no ENSO lag relationship is discernible in the NC mode, even though it appears strongly in the CB mode.

5. SIMULATIONS

5.1. Experimental design

Since the leading mode of early season rainfall exhibits the anticipated ENSO signal, the rest of the paper, by way of a model study, examines the mechanism by which the warm/cold ENSO-induced spring anomalies in the Caribbean yield the wet/dry early season rainfall anomalies. At the core of the numerical experiments are two control simulations based on Caribbean climate conditions in 1993 and 1989. Whereas 1993 saw the Caribbean region characterized by wet conditions, the region in 1989 was dry. For each control simulation the model was run over a 7 month period commencing in February, with boundary (SST and sea ice) and initial atmospheric conditions for the same year also prescribed.

The remaining experiments were simulations identical to the control runs, except that the boundary conditions (but not initial conditions) were replaced by those of different 'hot' and 'cold' years. 'Hot' years (determined by analysis of the GISST forcing dataset) were defined as those in which positive SSTAs existed in both the Caribbean in AMJ, and in the NINO3 and NINO4 regions the preceding November–March, i.e. 'hot' years exemplified tropical Atlantic and equatorial Pacific SST conditions consistent with positive early season rainfall departures in the CB region. The hot years chosen were 1958, 1969 and 1993 (Figure 6(a)–(c)). 'Cold' years, on the other hand, were oppositely defined, i.e. those in which negative SSTAs existed in both the Caribbean in AMJ, and in the NINO3 and NINO4 regions for the preceding November–March. 'Cold' years, therefore, exemplified SST conditions that would be expected to yield negative early season rainfall departures in the CB region. The cold years chosen were 1974, 1985 and 1989 (Figure 6(d)–(f)).

Note that each of our control year simulations is either a hot (1993) or cold (1989) year. The years 1993 and 1989 were chosen as the control simulations as, on average, over the early rainfall season they exhibited the smallest positive and negative Caribbean SST deviations respectively. The effect of applying marginally higher SSTA boundary conditions of the same sign, as well as those of opposite sign, could therefore be investigated.

We present results from two batches of five simulations. In the first (second) the initial conditions for 1993 (1989) were retained but the boundary conditions were successively replaced by those of the remaining two hot (cold) years and the three cold (hot) years. If, as is summarized, the SSTs of the NTA are as important in the generation of Caribbean rainfall anomalies, then the use of cold-year boundary conditions on 1993 initial conditions should result in a significant drying of the simulated Caribbean region (due to the colder SSTs in AMJ) in the first batch of experiments. The opposite should also be true of the use of hot-year boundary and 1989 initial conditions in the second batch of experiments.

The ten experiments are summarized in Table III. In order to differentiate the simulations, an identifier consisting of a letter, four digits and a second letter is used. The first two digits denote the control year (i.e. 1989 or 1993) with the preceding letter (W or D) indicating its status as a wet or dry Caribbean year. The next two digits indicate the year of forcing SST, and the final letter (H or C) denotes whether the forcing SST year is a hot (warm AMJ Caribbean SST) or cold (cool AMJ Caribbean SST). Hence W9374 C denotes a simulation using initial conditions of the wet year 1993 but with boundary conditions from the 'cold' year of 1974.

5.2. Precipitation

We first examine the simulated rainfall for evidence of an early season sensitivity to warm NTA SSTAs. Figure 7 shows the monthly values of the simulated area-averaged rainfall over the Caribbean for the two experiment batches. The averaging domain is the same as that used in the data study for the CSST index. The left panels (Figure 7(a)) show the 1993 simulations with hot- and cold-year boundary conditions imposed, and the right panels shows the same but for the 1989 simulations. In each panel the control simulation is shown

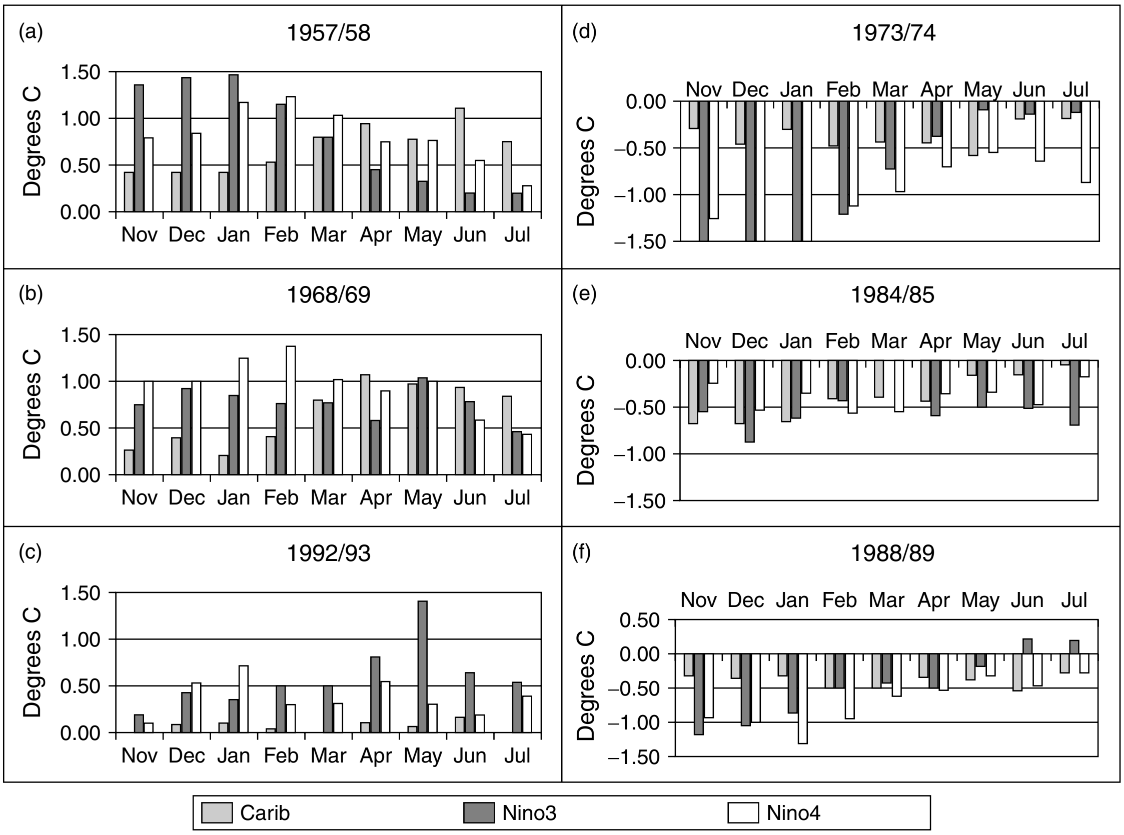

Figure 6. Carib, NINO3 and NINO4 SSTAs during (a)–(c) 'hot' years (1958, 1969 and 1993), (d)–(f) 'cold' years (1974, 1985 and 1989)

Table III. Numerical experiments. The identifiers in the table denote simulations in which the initial conditions were those of 1 February of the column year and the simulations are separated by rows into 'hot' and 'cold' forcing conditions (see text for explanation)

Simulation	1993	1989
Hot	W9393H — control simulation	D8958H
	W9358H	D8969H
	W9369H	D8993H
Cold	W9374C	D8989 C — control simulation
	W9385C	D8974 C
	W9389C	D8985C

first (grey bar) and, for comparison, the observed precipitation for the control year shown last (white). The model correctly simulates 1993 to be a wetter year than 1989, though it overpredicts the monthly precipitation amounts. In each panel, the simulated rainfall under hot-year conditions is shown as hatched bars; for cold-year conditions the bars are speckled.

Both the left and right panels confirm the effect of imposed warm and cold SSTs on early season Caribbean rainfall. In the left panels, the imposition of hot-year boundary conditions (9358 and 9369) on wet initial conditions results in early season rainfall amounts comparable to the wet 1993 control simulation. In all

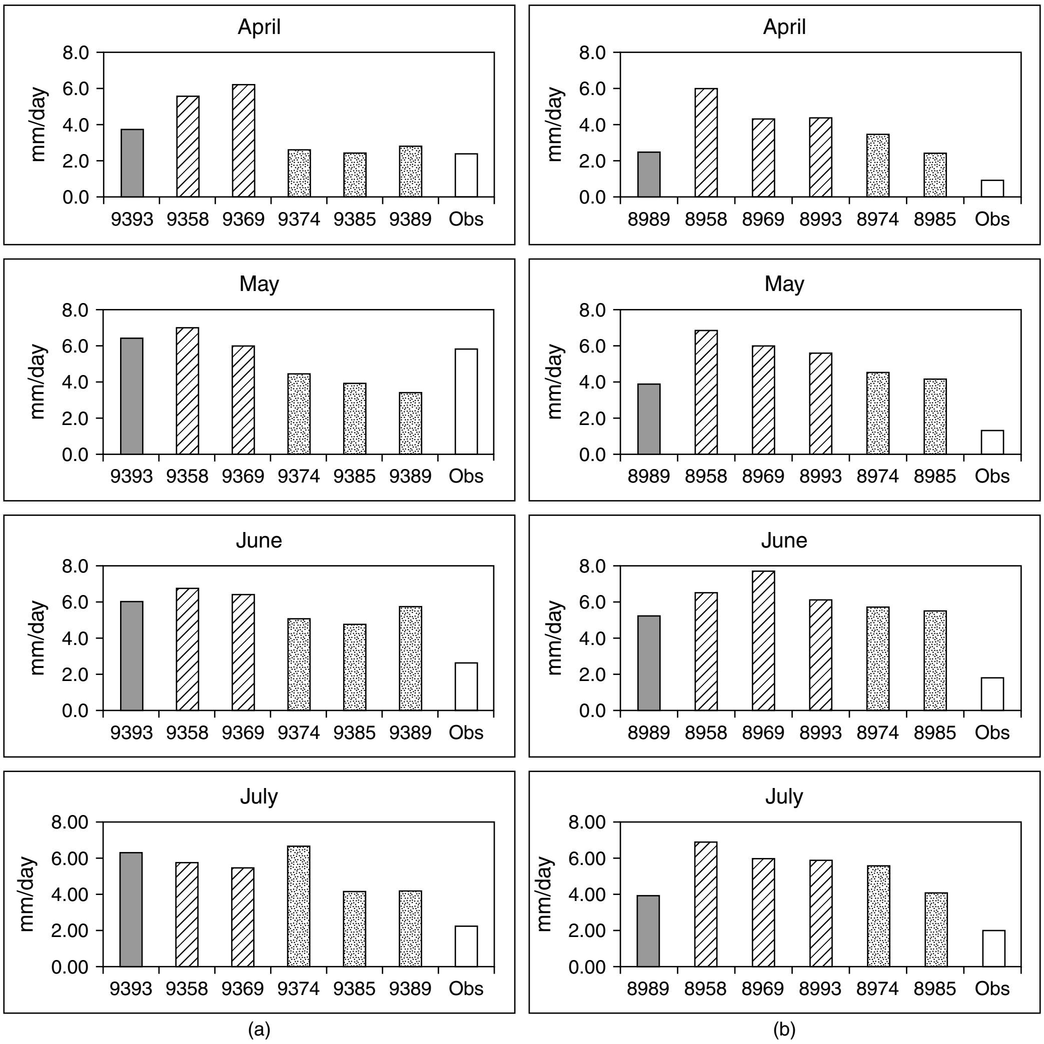

Figure 7. Mean monthly values of simulated precipitation (mm day^{-1}) area-averaged over the Caribbean basin for (a) the 1993 and (b) the 1989 experiments. The control simulations ('wet' 9393 and 'dry' 8989) and the observed precipitation for each month of the control years are given by the first and last bar in each graph

cases, with the exception of the 9374 simulation in July, these amounts exceed those for the corresponding simulations with cold-year boundary conditions (9374, 9385 and 9389). The pattern is repeated in the right panels, which similarly show the simulated rainfall for hot-year boundary conditions to exceed that of (i) the dry 1989 control simulation and (ii) the years with cold-year boundary conditions imposed. Though Figure 7 includes results for July (to show the above trends), the month of July is omitted from the remaining analysis. This is due to our previously stated lack of confidence in the model's ability to simulate this month reliably .

The left panels of Figure 8(a), (c) and (e), show respectively the composite April, May and June rainfall for experiments W9374C, W9385C and W9389C from which the corresponding monthly values for the wet control run (W9393H) have been subtracted. The panels, therefore, show the difference in simulated rainfall amounts during the early rainfall season due to the imposition of cool SSTs on a previously wet Caribbean. Likewise, the right panels, (b), (d) and (f), depict the composites when warm SSTs are imposed on a previously dry Caribbean. The panels reinforce the results of Figure 7: forcing with cold SSTs results in less rainfall than in the wet 1993 control simulations (left-hand panels), whereas forcing with SST from hot years yields more precipitation than in the dry 1989 control simulation (right-hand panels). The largest differences occur in May. This is consistent with the observed data, which show that the greatest difference between 1993 and 1989 precipitation occurred in May (Figure 7). It is also coincident with the period of largest ENSO-induced NTA SST change (Curtis and Hastenrath, 1995).

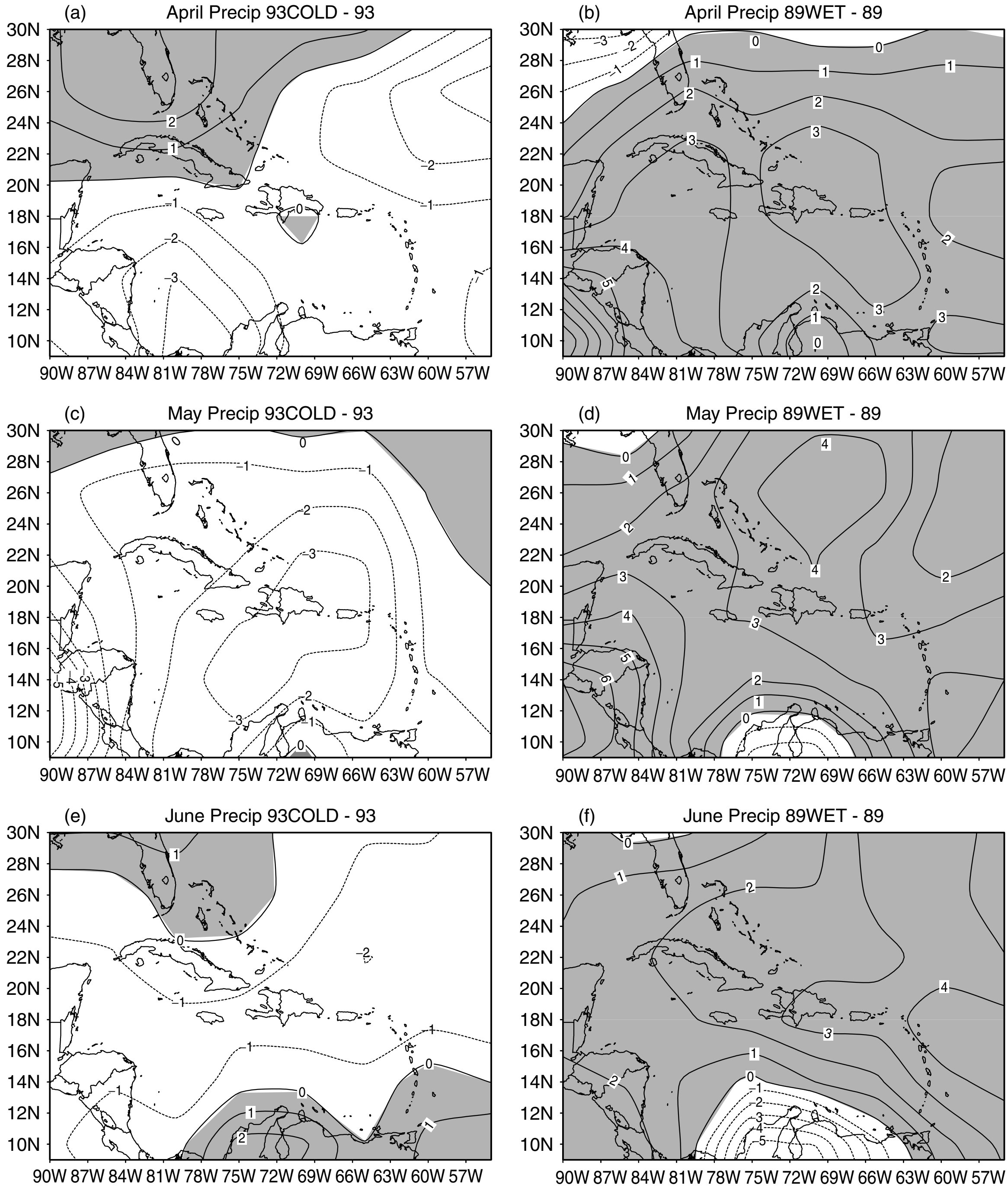

Figure 8. Composite April, May and June rainfall differences for hot- and cold-year simulations relative to the control years. Positive differences are shaded and the contour interval is 1 mm day^{-1}

Figure 8 also shows that for the selected warm/cold configuration of boundary conditions the resulting increase/decrease in mean rainfall amounts over the period is basinwide. The model captures the tendency for the northern Caribbean–south Florida to be excluded from the initiated SST effects, though on average it places the demarcation latitude much higher than that indicated by the EOF analysis of Section 4.

6. THE LARGE-SCALE CIRCULATION

To examine how the large-scale circulation is altered in the presence of the warm/cold early season SSTAs, similar diagrams to Figure 8 are generated for selected atmospheric variables. Figure 9 and Figure 10 respectively depict diagrams for sea-level pressure and surface temperature.

Both Figures 9 and 10 show significant differences between the left and right panels, suggesting a modification of both climatic variables due to the varying SST boundary conditions. Higher than normal surface pressures characterize the Caribbean basin during periods of anomalously cold NTA SSTs, as indicated by the positive differences in Figure 9(a), (c) and (e). The converse of lower surface pressures is also true for the imposition of hot-year boundary conditions on initial conditions corresponding to the dry 1989 (Figure 9(b), (d) and (f)). Cold NTA boundary conditions are also associated, on average, with cooler near-surface temperatures (Figures 10(a), (c) and (e)), with again the opposite being true for hot-year boundary conditions (Figure 10(b), (d) and (f)). (A warm lower atmosphere would contribute to decreased tropospheric stability over the region and *vice versa*.) For each panel of Figure 10 there also exists a demarcation latitude between regions of positive and negative surface temperature differences, with the north Caribbean and the Caribbean basin behaving roughly in anti-phase. The same is not true of the sea-level pressure panels (Figure 9).

Figure 11 shows the composites of simulated early season velocity potential near the surface (850 hPa) and aloft (200 hPa) for the cold- (panels (a) and (b)) and hot-year (panels (c) and (d)) simulations. The panels are averages for April through to June and represent large-scale circulation divergence tendencies for the early season. When cold-year SST boundary conditions are imposed in the ‘wet’ 1993 experiments, the Caribbean, on average, over the early season becomes divergent below and convergent aloft (Figure 11(a) and (b)). By contrast, the region becomes on average convergent below and divergent aloft when warm SSTs are imposed on a previously dry Caribbean (Figure 11(c) and (d)). In both instances the simulation results represent a change from the state of the Caribbean region during the control simulations.

Finally, Figure 12(a) and (b) shows the change in early season zonal wind shear that results from the imposition of a warm and cold Caribbean anomaly respectively. We include a wind shear diagram because of its importance to the development of tropical systems that traverse the region. Shear is defined as the difference between the zonal wind strengths at 200 and 850 hPa and the plots represent the mean difference in zonal shear between hot- and cold-year SST simulations using both 1993 (top) and 1989 (bottom) initial conditions. Areas where the composite vertical shear in the dry simulations is greater than that in the wet simulations are shaded. Figure 12 shows that when the Caribbean for both 1993 and 1989 initial conditions is dry (i.e. due to cold imposed SSTs) the mean vertical shear over the basin (but not over the north Caribbean) is larger. Note again that the demarcation between regions of positive and negative shear departures during periods of SST anomalies in the tropical Atlantic falls just south of 20 °N.

The patterns of Figure 9–12 indicate that when the NTA SST boundary conditions change from cold to warm, early season rainfall totals are not only greater (Figure 7), but the Caribbean region is characterized by lower surface pressures, warmer atmospheric surface temperatures (decreased stability), low-level convergence, upper-level divergence, and decreased vertical shear. The opposite is true for a change in SST conditions from warm to cold, which is coincident with a drying of the region. Knaff (1997), using data analysis, indicates tropospheric factors associated with greater Caribbean rainfall and major hurricane development. These include low surface pressure, low vertical shear, lower convective stability and warmer NTA SSTs. Figures 9–12 show patterns in tropospheric structure that are therefore consistent with a large-scale atmospheric circulation biased towards more (less) rain, in the presence of warm (cool) NTA SSTs.

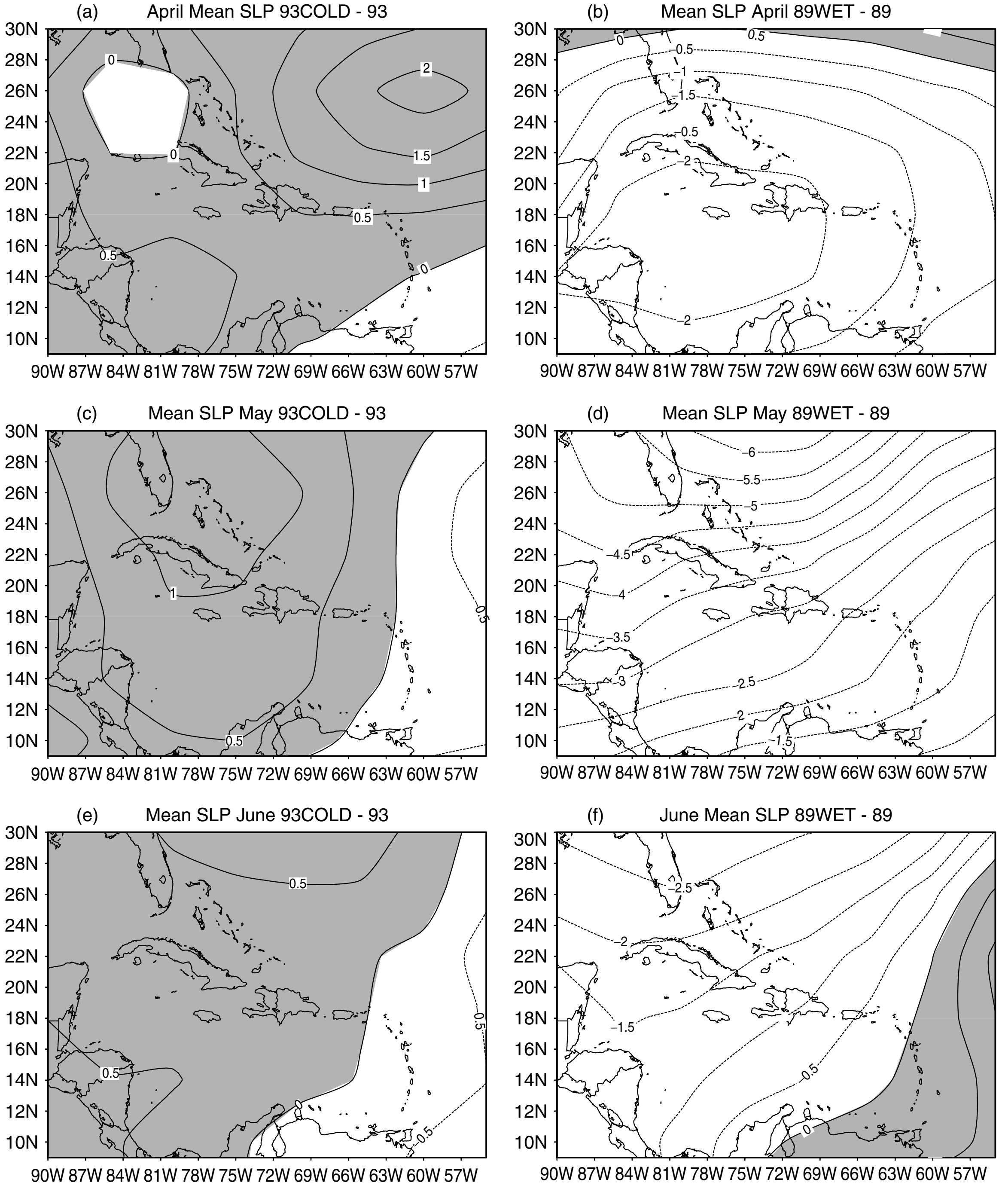

Figure 9. As for Figure 8, but for simulated sea-level pressure (SLP). Contour interval is 0.5 hPa

7. DISCUSSION

Goldenberg and Shapiro (1996) show that the development region for easterly waves is restricted to a narrow latitudinal band termed the main development region (MDR), between 10 and 20 °N. In April, the climatology of the Caribbean SST (not shown) is such that only the far western MDR (far western Caribbean Sea) possesses

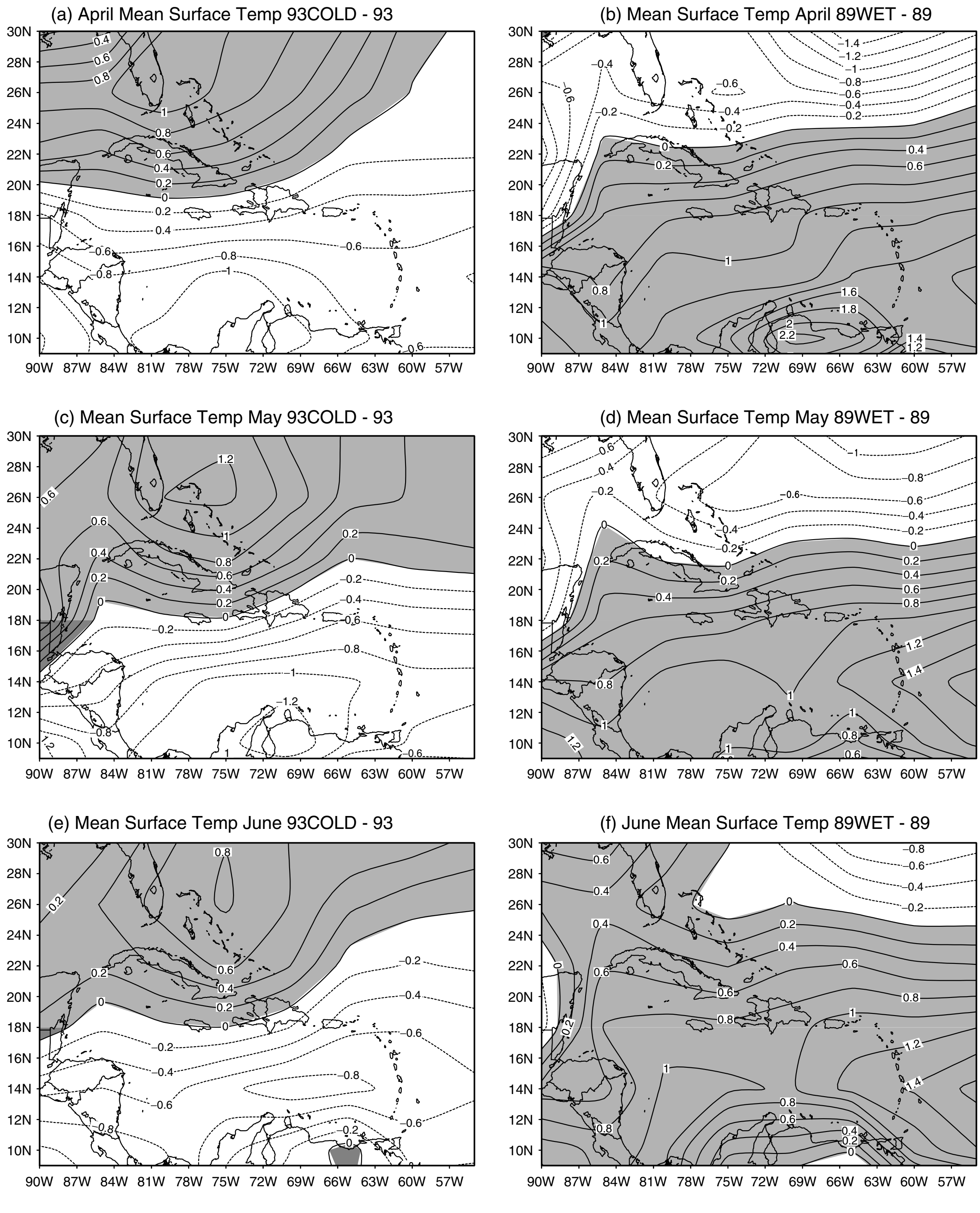

Figure 10. As for Figure 8, but for simulated mean simulated surface air temperature difference. Contour interval is 0.2 °C

SSTs in excess of 26.5 °C — the threshold for tropical convective development (Gray, 1968; Carlson, 1971; Emanuel, 1987). The appearance of positive NTA SSTAs of the order of 0.5 to 1 °C, as is the case in the El Niño+1 year (see Figure 6), would ensure that a larger portion of the MDR, and at least the Caribbean region, satisfied the SST criterion for convection. Therefore, the possibility exists for an earlier development of easterly waves in their westward track due to a shifting of the eastern edge of the Caribbean warm pool,

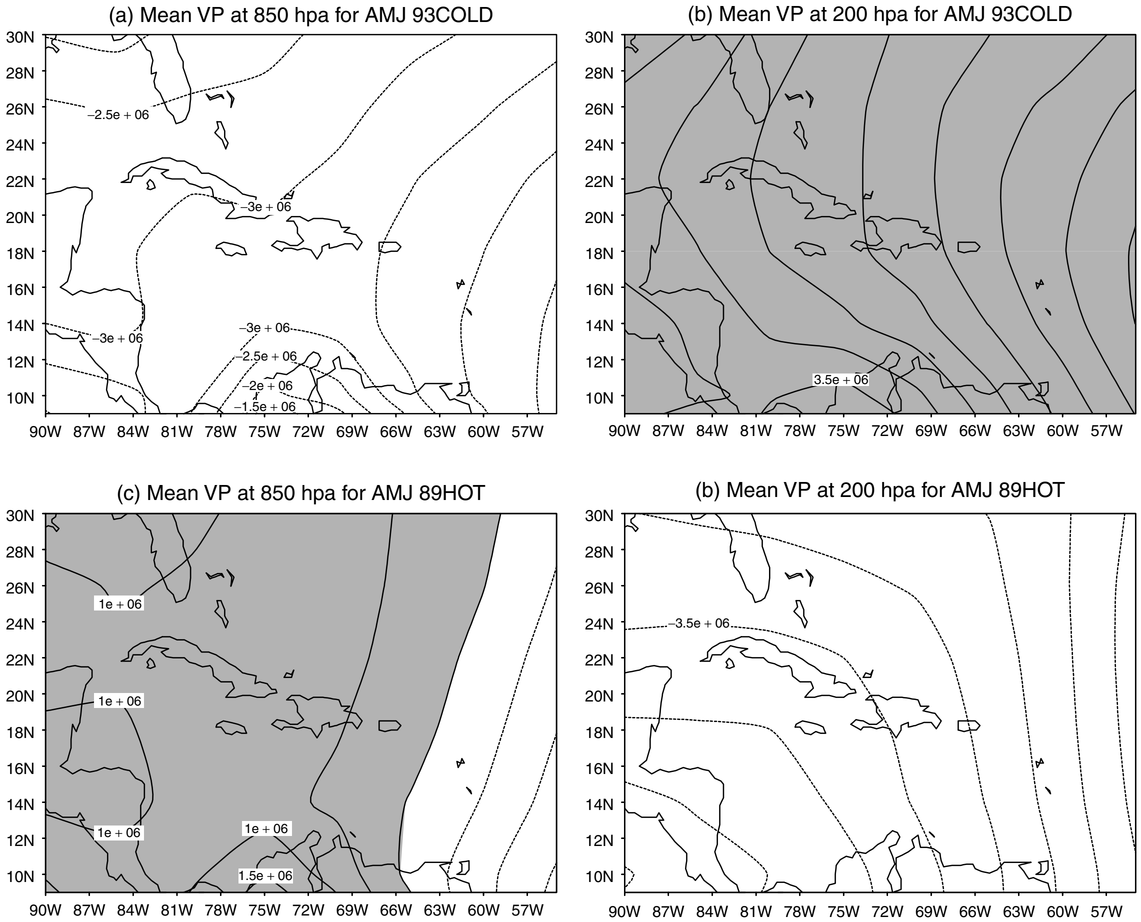

Figure 11. Composites of simulated early season velocity potential near the surface (850 hPa) and aloft (200 hPa) respectively for the 'cold' simulations with wet initial conditions (W93*xx*C) ((a) and (b)). (c) and (d) are as above but for 'hot' simulations with dry initial conditions (D89*xx*H). Positive values are shaded. Contour interval is 0.5×10^6 m^2 s^{-1}

and increased convective activity over the Caribbean during the early season. Since the warm anomalies are restricted to south of 20 °N, favourable conditions for convective development would not exist outside the MDR, likely accounting for the observed restriction of the early season rainfall anomalies to the Caribbean basin south of 20 °N in both model and data analysis.

Our simulations also showed that, though the entire region inclusive of southern Florida and northern Cuba possessed lower sea-level pressures and a conducive *convergence below–divergence aloft* pattern for a warm NTA (Figures 9 and 11), the simulated rainfall increases occurred only over that portion of the basin (south of 20 °N) where favourable shear (in addition to the warm SSTs) exists (Figures 10 and 12). The importance of low vertical shear to the development of Caribbean rainfall anomalies is implied.

Vertical shear is an equally important parameter for easterly wave development (Gray, 1968; Shapiro, 1982). Large shear magnitudes stifle the development of tropical convective systems even in the face of conducive SSTs below. (It is the strong shear during a warm equatorial Pacific event that likely accounts for the tendency for diminished rainfall during the peak Caribbean rainfall season.) This might also account for the restriction of rainfall anomalies to south of 20 °N, given that Figure 12 shows the Caribbean above that latitude to possess strong shear during warm NTA periods.

A known El Niño (La Niña) teleconnection in the Caribbean is that of an enhancement (diminution) of vertical shear via a strengthening (weakening) of the subtropical jet (Arkin, 1982; Shapiro, 1987; Aceituno,

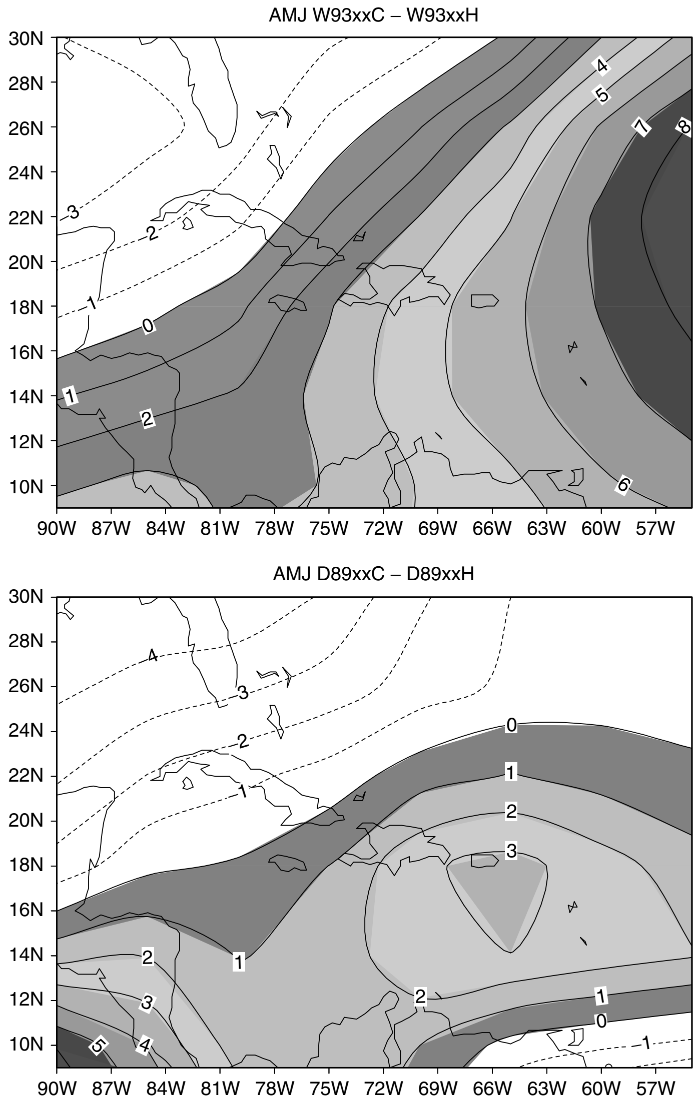

Figure 12. The difference between mean zonal wind shear for AMJ for cold and hot simulations for (a) 1993 and (b) 1989 initial conditions. Areas where the composite vertical shear for the dry simulations is greater than that for the wet simulations are shaded

1988b). During a warm tropical Atlantic–cool equatorial Pacific scenario (as would characterize an El Niño+1 year early season), low or near-normal vertical shear would characterize the Caribbean in addition to the warm NTA SSTAs. Ideal conditions would therefore exist over the Caribbean basin for tropical convective development, i.e. warm NTA SSTs and reduced vertical shear. This might suggest the bias toward early season rainfall anomalies during the El Niño+1 year.

8. CONCLUSION

Analysis of early season Caribbean precipitation data reveals a significant mode accounting for nearly half of its variability that is well correlated with equatorial Pacific anomalies one to two seasons before. The correlation is such that warm winter anomalies in the NINO3 and NINO4 regions are related to positive MJJ rainfall departures in the Caribbean basin south of 20 °N. The second leading mode for the northern Caribbean rainfall (south Florida and north Cuba) does not show a similar relationship with ENSO events.

We attribute the propagation of the warm ENSO event into the Caribbean early rainfall season to positive spring NTA SSTAs that develop in response to the wintertime equatorial Pacific anomalies. The leading mode, in addition to being correlated with winter Pacific SSTAs, also shows robust correlation with concurrent Caribbean SSTAs south of 20 °N, with warm anomalies associated with increased rainfall. The NC mode, on the other hand, is not significantly correlated with the NTA region of ENSO-induced spring SSTAs.

An AGCM is also utilized to show that, when warm Caribbean SSTAs akin to those seen in the El Niño+1 year are imposed, larger simulated rainfall totals occur during the early season. The converse is true for the imposition of cold SSTAs. The concurrent simulated state of the large-scale circulation for an increased early season rainfall is one characterized by lower than normal surface pressures, a warmer and convergent lower atmosphere, a divergent upper atmosphere and a low shear environment. These tropospheric conditions are consistent with a region biased towards more rain. As with the statistical analysis, the simulated increased rainfall due to warm Caribbean SSTs does not extend into the far north Caribbean.

The investigation suggests the need for further research on Caribbean rainfall variability. There is an obvious need for the running of a regional model centred over the Caribbean to study circulation changes on smaller spatial scales resulting from SST anomalies, including an investigation of the idea of more intense tropical waves developing under a warm NTA scenario. The idea of phases of the tropical Atlantic and Pacific being important for determining Caribbean rainfall also requires investigation, as little is known about how other configurations/scenarios, e.g. a warm Atlantic–warm Pacific, might alter Caribbean rainfall. Also puzzling is the difference between the model results and the analysis of observed data given in Figure 2. Model results suggest that the effects of ENSO-induced anomalies should be greatest in May, whereas Figure 2 shows that the greatest effect seems to occur in July. The dynamics of the MSD and its simulation by numerical models deserve further attention. Finally, the overwhelming decadal signal that characterized the two leading modes of early season Caribbean rainfall suggests a need to investigate the relationship between Caribbean rainfall and other global phenomena besides El Niño.

Intrinsic to all of the above is the importance of SST anomalies to Caribbean rainfall. SST anomalies in the tropics hold great potential for use as a predictor of extremes in tropical rainfall. This study suggests that spring SST anomalies that develop in the NTA due to an anomalous equatorial Pacific one or two seasons earlier, are useful for predicting precipitation departures in the Caribbean basin during the early rainfall season.

ACKNOWLEDGEMENTS

We acknowledge the assistance of the Center for Ocean Land Atmosphere Studies (COLA), Maryland, for assistance with the model, particularly J. Shukla and L. Marx, and of A. Roy for maintaining the COLA model. The research was partly funded by NSF grant number ATM-9815922 through the Inter American Institute (IAI) for Global Change, by the University of the West Indies (UWI) Fellowship Committee and by the Physics Department, UWI, through Dr P.N. Chin, Head.

REFERENCES

Aceituno P. 1988a. On the functioning of the Southern Oscillation in the South American sector. Part I: surface climate. *Monthly Weather Review* **116**: 505–524.

Aceituno P. 1988b. On the functioning of the Southern Oscillation in the South American sector. Part II: upper — air circulation. *Journal of Climate* **2**: 341–355.

Arkin PA. 1982. The relationship between the interannual variability in the 200 mb tropical wind field and the Southern Oscillation. *Monthly Weather Review* **110**: 1393–1401.

Brown P. 2000. *Third Caribbean Climate Outlook Forum*, Santo Domingo, May 3–5.

Carlson TN. 1971. An apparent relationship between the sea-surface temperature of the tropical Atlantic and the development of African disturbances into tropical storms. *Monthly Weather Review* **99**: 309–310.

Carton J, Huang B. 1994. Warm events in the tropical Atlantic Ocean. *Journal of Physical Oceanography*. **24**: 888–903.

Cattell RB. 1966. The scree test for the number of factors. *Multivariate Behavioral Research* **1**: 245–276.

Chang P, Ji L, Li H. 1997. A decadal climate variation in the tropical Atlantic Ocean from thermodynamic air–sea interactions. *Nature* **385**: 516–518.

Chen AA, McTavish J, Taylor M, Marx L. 1997. Using sea surface temperature anomalies to predict flood and drought conditions for the Caribbean. COLA Technical report No. 49: 24 pp.

Curtis S, Hastenrath S. 1995. Forcing of anomalous sea surface temperature evolution in the tropical Atlantic during Pacific warm events. *Journal of Geophysical Research* **100**: 15 835–15 847.

Ebisuzaki W. 1997. A method to estimate the statistical significance of a correlation when the data are serially correlated. *Journal of Climate* **10**: 2147–2153.

Emanuel KA. 1987. The dependence of hurricane intensity on climate. *Nature* **326**: 483–485.

Enfield DB, Mayer DA. 1997. Tropical Atlantic sea surface temperature variability and its relation to El Niño–Southern Oscillation. *Journal of Geophysical Research* **102**: 929–945.

Enfield DB, Alfaro EJ. 1999. The dependence of Caribbean rainfall on the interaction of the tropical Atlantic and Pacific oceans. *Journal of Climate* **12**: 2093–2103.

Fernandez B. 1996. Personal communication, Water Resources Authority, Jamaica.

Giannini A, Kushnir Y, Cane MA. 2000. Interannual variability of Caribbean rainfall, ENSO and the Atlantic Ocean. *Journal of Climate* **13**: 297–311.

Goldenberg SB, Shapiro LJ. 1996. Physical mechanism for the association of El Niño and West African rainfall with major hurricane activity. *Journal of Climate* **9**: 1169–1187.

Gray WM. 1968. Global view of the origin of tropical disturbances and storms. *Monthly Weather Review* **96**: 669–700.

Hastenrath S. 1976. Variations in the low-latitude circulation and extreme climatic events in the tropical Americas. *Journal of Atmospheric Science*. **33**: 202–215.

Houghton RW, Tourre YM. 1992. Characteristics of low-frequency sea surface temperature fluctuations in the tropical Atlantic. *Journal of Climate* **5**: 765–771.

Kaiser HF. 1960. The application of electronic computers to factor analysis. *Educational and Psychological Measurements* **20**: 141–151.

Kinter III JL, Shukla J, Marx L, Schneider EK. 1988. A simulation of the winter and summer circulations with the NMC Global Spectral Model. *Journal of Atmospheric Science* **45**: 2486–2522.

Knaff JA. 1997. Implications of summertime sea level pressure anomalies in the tropical Atlantic region. *Journal of Climate* **10**: 789–804.

Kutzbach JE. 1967. Empirical eigenvectors of sea-level pressure, surface temperature and precipitation complexes over North America. *Journal of Applied Meteorology* **6**: 791–802.

Magaña V, Amador JA, Medina S. 1999. The mid-summer drought over Mexico and Central America. *Journal of Climate* **12**: 1577–1588.

Mehta VM, Delworth T. 1998. Variability of the tropical ocean surface temperatures at decadal–multidecadal timescales. Part I: the Atlantic. *Journal of Climate* **11**: 2351–2375.

Parker DE, Folland CK, Brevan A, Ward MN, Jackson M, Maskell K. 1995. Marine surface data for analysis of climate fluctuations on interannual to century time scales, In *Natural Climate Variability on Decade-to-Century Time Scales*, Martinson DG, Bryan K, Ghil M, Hall MM, Karl TR, Satachik ES, Sorooshian S, Talley LD (eds). National Academic Press: Washington, DC.

Reynolds RW. 1988. A real-time global SST analysis. *Journal of Climate* **1**: 75–86.

Rogers JC. 1988. Precipitation variability over the Caribbean and tropical Americas associated with the Southern Oscillation. *Journal of Climate* **1**: 172–182.

Ropelewski CF, Halpert MS. 1986. North American precipitation and temperature patterns associated with the El Niño/Southern Oscillation. *Monthly Weather Review* **114**: 2352–2362.

Ropelewski CF, Halpert MS. 1987. Global and regional scale precipitation patterns associated with the El Niño/Southern Oscillation. *Monthly Weather Review* **115**: 1606–1626.

Ropelewski CF, Halpert MS. 1989. Precipitation patterns associated with the high index phase of the southern oscillation. *Journal of Climate* **2**: 268–284.

Ropelewski CF, Halpert MS. 1996. Quantifying southern oscillation–precipitation relationships. *Journal of Climate* **9**: 1043–1059.

Sela JG. 1980. Spectral modeling at the National Meteorological Center. *Monthly Weather Review* **108**: 1279–1292.

Shapiro LJ. 1982. Hurricane climatic fluctuations. Part I: patterns and cycle. *Monthly Weather Review* **110**: 1007–1013.

Shapiro LJ. 1987. Month-to-month variability of the Atlantic tropical circulation and its relationship to tropical storm formation. *Monthly Weather Review* **125**: 2598–2614.

Shukla J. 1993. Predictability of short term climate variations. *Prediction of Interannual Climate Variations*. Shukla J (ed.). *NATO ASI Series, Vol. 16.* Springer-Verlag: Berlin, Heidelberg; 217–231.

Shukla J, Fennessy MJ. 1988. Prediction of time-mean atmospheric circulation and rainfall: influence of Pacific sea surface temperature anomaly. *Journal of Atmospheric Science* **45**: 9–28.

Taylor M. 1996. Validating a general circulation model for use within the Caribbean. M.Phil. thesis, University of the West Indies.

Taylor M. 1999. October in May: the effect of warm tropical Atlantic SSTs on early season Caribbean rainfall. Ph.D. thesis, University of Maryland, College Park.

Vose RS, Schmoyer PM, Steurer PM, Peterson TC, Heim R, Karl TR, Eischeid JK. 1992. The Global Historical Climatology Network, Environmental Sciences Division, Publication No. 3912. United States Department of Energy; 1–99.

Xie P, Arkin P. 1997. Global precipitation: a 17-year monthly analysis based on observations, satellite estimates and numerical model outputs. *Bulletin of the American Meteorological Society* **78**: 2539–2558.

Xue Y, Sellers P, Kinter J, Shukla J. 1991. A simplified biosphere model for global climate studies. *Journal of Climate* **4**: 345–364.

